

## MULTIWAVELENGTH SED AS A TOOL IN UNDERSTANDING OUTBURSTS OF SYMBIOTIC BINARIES

A. Skopal

*Astronomical Institute, Slovak Academy of Sciences, 059 60 Tatranská  
Lomnica, Slovakia; skopal@ta3.sk*

Received: 2011 September 1; accepted: 2011 September 15

**Abstract.** Symbiotic binaries consist of a few sources of radiation contributing to spectral energy distribution (SED) from hard X-rays to radio wavelengths. To identify the basic physical processes forming the observed spectrum, we have to disentangle the composite SED into its individual components of radiation, i.e., to determine their physical parameters. Spectral disentangling of different objects at different stages of activity allows us to understand the mechanism of their outbursts. In this contribution I demonstrate the method of multiwavelength modeling SEDs on the example of two classical symbiotic stars, AG Dra and Z And.

**Key words:** stars: binaries: symbiotic – X-rays: binaries – stars: fundamental parameters

### 1. INTRODUCTION

Symbiotic stars are interacting binary systems consisting of a cool giant and a hot compact star – in most cases a white dwarf (WD). Typical orbital periods are between 1 and 3 years, but can be significantly larger.

There are two principal processes of interaction between the components. (1) Mass loss from the cool component in the form of a wind, which is primary condition for the appearance of the symbiotic phenomenon, and (2) accretion of a part of the material lost by the giant by its compact companion. The latter generates a very hot ( $T_h \approx 10^5$  K) and luminous ( $L_h \approx 10^2 - 10^4 L_\odot$ ) source of radiation, which is capable of ionizing the circumbinary material giving rise to *nebular* emission. As a result the spectrum of symbiotic stars consists of three basic components of radiation – two stellar (from the binary components) and one nebular, emitted primarily by the ionized wind from the giant.

The very large range in the energy output from the accretor is caused by the two different mechanisms. In rare cases, the hot star luminosity of 10–100  $L_\odot$  can be powered solely by the accretion onto a WD (e.g., EG And and 4 Dra, see Skopal 2005a), while in most cases the observed luminosities,  $10^3 - 10^4 L_\odot$ , are believed to be caused by a stable hydrogen nuclear burning on the surface of WD (e.g., Paczyński & Żytkow 1978). Considering the activity, two basic stages of a symbiotic binary are distinguishable – a quiescent and an active phases.

### 1.1. Quiescent phase

If the processes of the mass-loss, accretion and ionization are in a mutual equilibrium, then the symbiotic system releases its energy approximately at constant rate. This stage is called as the *quiescent phase*. Taking into account the principal processes acting in symbiotic stars, the nebular radiation during quiescent phases originates in a fraction of the giant's wind, ionized by the hot component. Based on this assumption, Seaquist et al. (1984) first treated the equilibrium condition between the rate of ionizing photons and recombinations in the ionized wind from the giant for pure hydrogen gas and the steady state situation. With this model they successfully explained the radio emission from symbiotic stars. This view was confirmed directly by Nussbaumer et al. (1988), who found that symbiotic objects best fit the CNO abundance ratios of normal red giants, which thus strongly support the idea that quiescent symbiotics are binaries, in which a hot ionizing source illuminates the stellar material of a red giant star. The presence of an extended and partially optically thick nebula in symbiotic systems causes the wave-like, orbitally-related light variation, which is the most typical feature seen in the light curves of symbiotic stars during their quiescent phases (e.g. Belyakina 1979; Skopal 2008; Jurđana-Šepić & Munari 2010).

Modeling the spectral energy distributions (hereafter SEDs) from the ultraviolet to the near-IR shows that the hot star continuum dominates in the far-UV, the nebular component is most pronounced in the near-UV and the short-wavelength optical range, while the giant's photosphere gives the main input in the optical range – from the *V* passband to the near infrared (e.g., Kenyon & Webbink 1984; Mürset et al. 1991; Skopal 2005b). However, outbursts of symbiotic stars change the situation considerably.

### 1.2. Active phase

Once the equilibrium between the principal processes is disturbed, symbiotic system changes its radiation significantly – brightens up in the optical by a few magnitudes and its SED signals a dramatic change in the ionization structure of the binary. The star's brightening is followed by enhanced mass-outflow from the hot star for a few months to years. We name this stage as the *active phase*.

The event of outbursts could result from an increase in the accretion rate above that sustaining the stable burning, which leads to expansion of the burning envelope to an A–F type (pseudo)photosphere (e.g., Tutukov & Yangelson 1976). As a result, the pseudophotosphere will radiate at a lower temperature, and this shifts the maximum of its SED to longer wavelengths, causing a brightening in the optical. Based on optical observations, this scenario was supported by many authors. Recently, Siviero et al. (2009) applied it for the 2008–2009 active phase of CI Cyg. However, modeling SED in the UV/near-IR continuum of symbiotic binaries with a high orbital inclination during the active phases, indicated an increase of *both* the stellar radiation from a warm ( $1\text{--}2 \times 10^4$  K) pseudophotosphere and the nebular emission. This led to suggestion that there is an edge-on disk around the accretor, the outer flared rim of which simulates the warm pseudophotosphere, and the nebula is placed above/below the disk (Skopal 2005b). A significant change in the light curve profile, from a broad wave to a narrow minimum (eclipse) during the transition from the quiescent to active phase (e.g., Belyakina 1991), supports this interpretation independently. In addition, this also signals a dramatic change in the ionization structure in the binary, because a considerable part of the hot

component radiation is a subject to eclipse, in contrast to quiescence, when the hot component contribution to the optical is negligible.

The key problem in the research of symbiotic stars is understanding the nature of their outbursts. However, their puzzling character precludes a standard explanation. Here, I use the method of multiwavelength modeling of their SEDs to reconstruct the spectra observed during quiescence and activity. This can help to identify the responsible physical processes and achieve a better understanding of the nature of their outbursts.

## 2. MULTIWAVELENGTH MODELING THE SED

According to the basic properties of symbiotic stars, as described in Section 1, the composite spectrum emitted by symbiotic stars,  $F(\lambda)$ , can formally be expressed as a superposition of its three basic components, i.e.,

$$F(\lambda) = F_h(\lambda) + F_n(\lambda) + F_g(\lambda), \quad (1)$$

where  $F_h(\lambda)$ ,  $F_n(\lambda)$  and  $F_g(\lambda)$  represent radiative contributions from the hot stellar source, nebula and giant, respectively.

For the sake of simplicity, and with respect to the current modeling the low-resolution X-ray data, I approximate the hot stellar continuum by a blackbody at the temperature  $T_h$ , the nebular radiation in the continuum by processes of recombination and thermal bremsstrahlung in the hydrogen plasma for Case B (i.e. optically thick in the Lyman continuum), and the radiation from the giant by a synthetic spectrum,  $F_\lambda^{\text{synth.}}(T_{\text{eff}})$  (models from Hauschildt et al. 1999). Then Equation (1) can be written in a form,

$$F(\lambda) = \theta_h^2 \pi B_\lambda(T_h) e^{-\sigma_X(\lambda) N_H} + k_n \varepsilon_\lambda(H, T_e) + \theta_g^2 F_\lambda^{\text{synth.}}(T_{\text{eff}}), \quad (2)$$

where scalings  $\theta_h = R_h/d$  and  $\theta_g = R_g/d$  represent angular radii of the emitting spherical photospheres of the hot star and the giant, respectively. The factor  $k_n$  [ $\text{cm}^{-5}$ ] scales the volume emission coefficient  $\varepsilon_\lambda(T_e)$  [ $\text{erg cm}^3 \text{s}^{-1} \text{\AA}^{-1}$ ] of the nebular continuum to observations. Further, the electron temperature,  $T_e$ , and thus  $\varepsilon_\lambda(T_e)$  were assumed to be constant throughout the nebula, which simplifies determination of the emission measure of the nebula to  $EM = 4\pi d^2 k_n \text{ cm}^{-3}$  (Skopal 2005b). The observed X-ray fluxes are attenuated by b-f absorptions.  $N_H$  is the total hydrogen column density [ $\text{cm}^{-2}$ ] and  $\sigma_X(\lambda)$  [ $\text{cm}^2$ ] is the total cross-section for photoelectric absorption per hydrogen atom (Cruddace et al. 1974). Here, I used the *tbabs* absorption model for interstellar matter composition with abundances given by Wilms et al. (2000).

In the SED-fitting analysis, theoretical fluxes of the composite continuum (Eq. 2) were fitted to the measured fluxes. They consist of the *observed* X-ray fluxes and *dereddened* UV/optical/IR fluxes. To simplify the task, contribution of the giant,  $F_g(\lambda)$ , which dominates the near-IR, was subtracted. Parameters of this component,  $\theta_g$  and  $T_{\text{eff}}$ , were estimated by comparing an appropriate synthetic spectrum to the photometric (*VR*)*IJHK* flux points. Other fitting parameters can be obtained from a grid of models for reasonable ranges of the model variables ( $\theta_h$ ,  $T_h$  and  $N_H$  for the hot stellar source, and  $T_e$  and  $k_n$  for the nebular continuum), which correspond to a minimum of the reduced  $\chi^2$  function. If the errors of measured fluxes are not available, they can be put to canonical values of 10%.

More details about modeling the multiwavelength SEDs of symbiotic stars can be found in Skopal (2005b) and Skopal et al. (2009a).

### 3. EXAMPLE OBJECTS

#### 3.1. *AG Draconis*

AG Dra is a yellow symbiotic binary comprising a K2 III giant (Mürset & Schmid 1999) and a WD accreting wind from the giant on a 549-day orbit (Fekel et al. 2000). AG Dra is non-eclipsing binary (e.g. Mikolajewska et. 1995). The light curve of AG Dra shows numerous short-term bursts with amplitudes of 1–3 mag in  $U$  (Figure 1). The latest, 2006–2008 major outburst was described by Munari et al. (2009) and Shore et al. (2010).

During outbursts, a strong increase in the nebular component of radiation and indication of an enhanced stellar wind from the hot star, were observed (Tomov & Tomova 2002; Leedjävrv et al. 2004). A significant contribution from the nebula in the near-UV/optical and its strengthening during outbursts was confirmed independently by modeling the UV/IR continuum (Skopal 2005b).

AG Dra produces a strong supersoft X-ray emission. Greiner et al. (1997) first noted a variation in the X-ray fluxes that are in anticorrelation to those in the UV and the optical. The X-ray history of AG Dra has recently been reviewed by González-Riestra et al. (2008), who found that this anticorrelation appears to be a general feature of AG Dra radiation and is independent of the type and strength of the outburst.

Here I briefly introduce the origin of the observed X-ray/optical-UV flux anticorrelation on the basis of the multiwavelength modeling the SED from the supersoft X-rays to the near-IR during the 2003 burst (XMM-Newton observations from 2003/10/10, FUSE observations from 2003/11/14) and the following quiescent phase (XMM-Newton observation from 2004/06/15, FUSE observations from 2004/06/24). Main results can be summarized as follows.

(1) During the quiescent phase the radiation of the hot component can be reproduced by a black body with a radius  $R_h = 0.031(d/1.1\text{kpc}) R_\odot$ , radiating at the temperature  $T_h = 164\,400$  K, which yields the luminosity  $L_h = 630(d/1.1\text{kpc})^2 L_\odot$ . The X-ray emission was attenuated by absorptions parametrized with  $N_H = 2.82 \times 10^{20} \text{ cm}^{-2}$ , which is equivalent to its *interstellar* value. The emission measure of the nebular component of radiation was  $EM = 1.3 \times 10^{59} (d/1.1\text{kpc})^2 \text{ cm}^{-3}$ . The star's brightness was as low as  $U \approx 11$ , and the O VI 1032, 1038 Å wings were faint, corresponding to the electron optical depth of  $\sim 0.06$  (Figure 1, right panels).

(2) During the 2003 burst, a high value of  $T_h \geq 180\,000$  K and  $L_h \geq 1760 (d/1.1\text{kpc})^2 L_\odot$ , are required to reproduce the observed large amount of  $EM = 6.2 \times 10^{59} (d/1.1\text{kpc})^2 \text{ cm}^{-3}$ . The negative detection of the supersoft X-ray emission constrains a significant absorption with  $N_H \geq 2.5 \times 10^{21} \text{ cm}^{-2}$ . The flux of the broad O VI 1032, 1038 Å wings was by a factor of  $\sim 2$  larger than during quiescence, and corresponded to a large electron optical depth of  $\sim 0.08$ . The star's brightness was as high as  $\sim 9.5$  (Figure 1, left panels).

First, the multiwavelength modeling the SED unambiguously confirmed the flux anticorrelation. Second, determining physical parameters of the radiative components, responsible for the observed anticorrelation, allowed us to propose its origin. The source of the opacity, causing the observed anticorrelation between

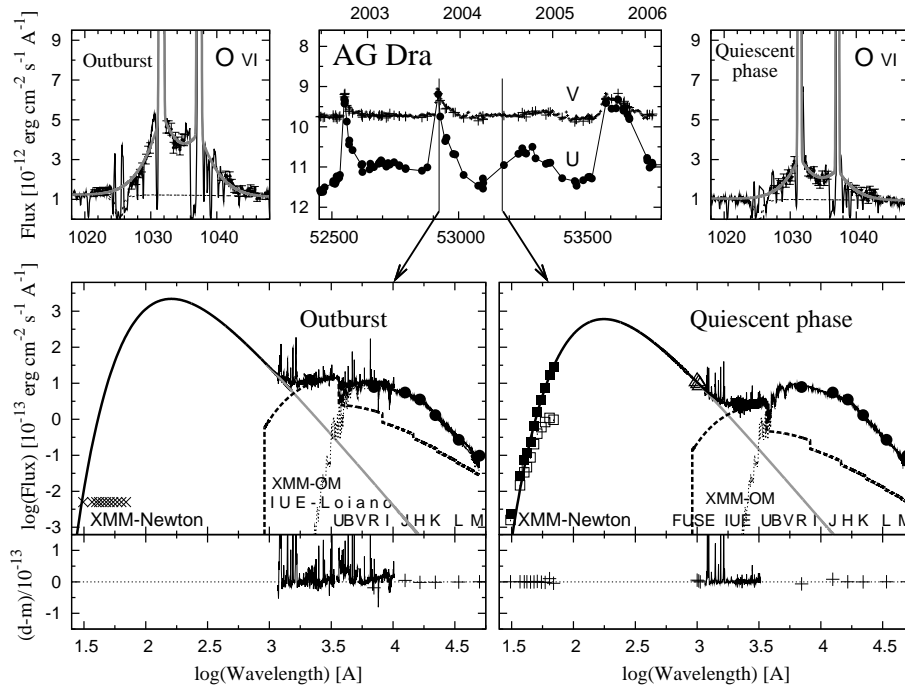


**Fig. 1.** Bottom: SEDs of the multiwavelength model of the AG Dra continuum during the 2003 burst (left) and the quiescence (right). The model SED (solid thick line) and its components (from the hot star in gray, the nebula as the broken line and the giant as the dotted line) represent the graphic form of Eq. (2). Corresponding  $U$  and  $V$  magnitudes are shown in the top mid panel, and the broad wings of the O VI 1032, 1038 Å lines are plotted at the top outer panels (adapted according to Figure 2 of Skopal et al. 2009a).

the X-ray and optical/UV fluxes, can be associated with the hot star wind, which is enhanced during the active phases of symbiotic binaries (e.g. Tomov & Tomova 2002 for AG Dra; Skopal 2006 in general). The higher mass-loss rate increases the particle density in the vicinity of the WD and thus the electron optical depth. This event increases the number of bound-free absorptions in the line of sight, which leads to a significant *attenuation* of the supersoft X-ray photons, and consequently, the free-bound transitions *increases* the nebular emission that dominates in the optical/near-UV. In other words, the injection of particles into the field of ionizing photons increases number of ionization/recombination acts resulting in a decrease of the original X-ray photons, whose energy is converted into the near-UV/optical as the nebular radiation. More details can be found in Skopal et al. (2009a).

### 3.2. *Z Andromedae*

*Z And* is considered as the prototype of a class of symbiotic stars. The binary is composed of a late-type, M4.5 III, giant and a WD, accreting from the giant's wind on the 759-day orbit (e.g. Fekel et al. 2000). Its recent activity started from 2000 September and reached the optical maxima in 2000 December, 2004 September, 2006 July, 2008 January/June and 2009 December (Figure 2). During all the well observed large eruptions, signatures of high-velocity outflows were detected



ment in Eq. (1), photospheric synthetic spectra of M-giant stars, as published by Fluks et al. (1994), were used. These models were calculated in the spectral range 350–900 nm for 11 spectral types, from M0 to M10.

The presence of F-G type features in the 2009/08/28 spectrum suggested the temperature of a stellar source to be as low as 5000–7000 K. Therefore, I compared the continuum of the hot stellar source to a synthetic spectrum, calculated for 5000–9000 K using the Kurucz codes (Munari et al. 2005). So, the first term of Eq. (1) can be written as

$$F_h(\lambda) = (\theta_{\text{warm}}^{\text{eff}})^2 \mathcal{F}_\lambda(T_{\text{eff}}), \quad (3)$$

where  $\mathcal{F}_\lambda(T_{\text{eff}})$  is the synthetic spectrum representing the warm stellar component of radiation. Its corresponding effective temperature,  $T_{\text{eff}}$ , and the scaling factor,  $\theta_{\text{warm}}^{\text{eff}} = R_{\text{warm}}^{\text{eff}}/d$ , represent free parameters in modeling the SED.

The 2009/08/28 spectrum was possible to reproduce by superposition of a warm pseudophotosphere ( $T_{\text{eff}} = 5300$  K,  $R_{\text{warm}}^{\text{eff}} = 11.4(d/1.5\text{kpc}) R_\odot$ , and  $L_h = 89(d/1.5\text{kpc})^2 L_\odot$ ), the nebular hydrogen continuum ( $T_e = 22000$  K,  $EM = 2.3 \times 10^{60}(d/1.5\text{kpc})^2 \text{cm}^{-3}$ ) and the giant photosphere with a spectral type of M4.4, corresponding to the effective temperature,  $T_{\text{eff}} = 3450$  K (see the left bottom panel in Figure 2). After 28 days only, on 2009/09/25, a dramatic change in the continuum profile was indicated. The warm pseudophotosphere was well reproduced by the blackbody with  $T_{\text{bb}} = 9000$  K,  $R_{\text{bb}}^{\text{eff}} = 12.9(d/1.5\text{kpc}) R_\odot$  and  $L_h = 978(d/1.5\text{kpc})^2 L_\odot$ , the contribution of which dominated the whole optical domain. The nebular component was rather faint, radiating at  $T_e \sim 30000$  K and having  $EM = 0.1 \times 10^{60}(d/1.5\text{kpc})^2 \text{cm}^{-3}$ . Contribution from the giant remained practically unchanged (see Figure 2 right bottom panel). Physical parameters of the warm stellar pseudophotosphere suggest that its shape cannot be spherical. If it were a sphere, its radiation would not be capable of giving rise the observed nebular emission. On the other hand, the presence of a strong nebular component in the spectrum constrains the presence of a hot ionizing source in the system. Such the composition of the spectrum suggests that there is a flared disk around the hot star, whose outer rim simulates the warm pseudophotosphere, while the region located above/below the disk can easily be ionized by the central hot star and thus produce a nebular emission. This suggestion requires a high orbital inclination of Z And ( $i \sim 75^\circ$ , see Skopal 2003; Isogai et al. 2010).

#### 4. CONCLUSION

In this contribution I have applied a method of multiwavelength modeling the SEDs of classical symbiotic stars AG Dra and Z And during different levels of their activity with the aim to identify the origin of the main changes in their spectrum. In the case of AG Dra the method demonstrated that the supersoft X-ray vs. optical/UV flux anticorrelation is caused by a variable wind from the hot star. The enhanced hot star wind gives rise to the optical bursts by reprocessing high-energy photons from the Lyman continuum to the optical/UV range. In the case of Z And, disentangling of its composite spectrum in the 2009 outburst identified a warm stellar source in the spectrum. The source had a form of a flared disk with outer rim simulated the warm pseudophotosphere. The ionized region was located above/below it giving rise to the nebular emission.

ACKNOWLEDGMENTS. This work was supported by the Slovak Academy of Sciences grant, VEGA No. 2/0038/10.

## REFERENCES

- Belyakina, T. S. 1979, *Izv. Crimean AO*, 59, 133  
 Belyakina, T. S. 1991, *Bull. Crimean AO*, 83, 104  
 Cruddace R., Paresce F., Bowyer S., Lampton M. 1974, *ApJ*, 187, 497  
 Fekel F. C., Hinkle K. H., Joyce R. R., Skrutskie, M. F. 2000, *AJ*, 120, 3255  
 Fernández-Castro T., González-Riestra R., Cassatella A. et al. 1995, *ApJ*, 442, 366  
 Fluks M. A., Plez B., Thé P. S. et al. 1994, *A&AS*, 105, 311  
 González-Riestra R., Viotti R. F., Iijima T. et al. 2008, *A&A*, 481, 725  
 Greiner J., Bickert K., Luthardt R. et al. 1997, *A&A*, 322, 576  
 Hauschildt P. H., Allard F., Ferguson J. et al. 1999, *ApJ*, 525, 871  
 Isogai M., Seki M., Ikeda Y., Akitaya H., Kawabata K. S. 2010, *AJ*, 140, 235  
 Jurdana-Šepić R., Munari U. 2010, *PASP*, 122, 35  
 Kenyon S. J., Webbink R. F. 1984, *ApJ*, 279, 252  
 Leedjävrv L., Burmeister M., Mikolajewski M. et al. 2004, *A&A*, 415, 273  
 Mikolajewska J., Kenyon S. J., Mikolajewski M. et al. 1995, *AJ*, 109, 1289  
 Munari U., Sordo R., Castelli F., Zwitter T. 2005, *A&A*, 442, 1127  
 Munari U., Siviero, A., Ochner P. et al. 2009, *PASP*, 121, 1070  
 Mürset U., Nussbaumer H., Schmid H. M., Vogel M. 1991, *A&A*, 248, 458  
 Mürset U., Schmid H. M. 1999, *A&AS*, 137, 473  
 Nussbaumer H., Schmid H. M., Vogel M., Schild H. 1988, *A&A*, 198, 179  
 Paczyński B., Żytkow A. N. 1978, *ApJ*, 222, 604  
 Seaquist E. R., Taylor A. R., Button S. 1984, *ApJ*, 284, 202  
 Siviero A., Munari U., Dallaporta S. et al. 2009, *MNRAS*, 399, 2139  
 Shore S., Wahlgren G. M., Genovali K. et al. 2010, *A&A*, 510, A70  
 Skopal A. 2003, *A&A*, 401, L17  
 Skopal A. 2005a, in *Cataclysmic Variables and Related Objects*, eds. P.-J. Lasota and M. Hammury, *ASP Conf. Ser.*, 330, 463  
 Skopal A. 2005b, *A&A*, 440, 995  
 Skopal A. 2006, *A&A*, 457, 1003  
 Skopal A. 2008, *JAAVSO*, 36, 9  
 Skopal A., Pribulla T. 2006, *ATel*, 882, 1  
 Skopal A., Vittone A. A., Errico L. et al. 2006, *A&A*, 453, 279  
 Skopal A., Sekeráš M., González-Riestra R., Viotti R. F. 2009a, *A&A*, 507, 1531  
 Skopal A., Pribulla T., Budaj J. et al. 2009b, *ApJ*, 690, 1222  
 Tomov N., Tomova M. 2002, *A&A*, 388, 202  
 Tarasova T. N., Skopal A. 2012, *Astron. Rep.*, 56, 218  
 Tutukov A. V., Yungelson L. R. 1976, *Astrofizika*, 12, 521  
 Wilms J., Allen A., McCray R. 2000, *ApJ*, 542, 914